

# Sinterability of $\beta$ -SiAlON powder prepared by carbothermal reduction and simultaneous nitridation of ultrafine powder in the $\text{Al}_2\text{O}_3$ - $\text{SiO}_2$ system

I. J. DAVIES\*, T. MINEMURA<sup>†</sup>, N. MIZUTANI<sup>‡</sup>, M. AIZAWA<sup>‡</sup>, K. ITATANI<sup>‡,§</sup>  
 Departments of \*Mechanical Engineering and <sup>‡</sup>Chemistry, Faculty of Science and Engineering, Sophia University, 7-1 Kioi-cho, Chiyoda-ku, Tokyo 102-8554, Japan  
 E-mail: itatani@hoffman.cc.sophia.ac.jp

Three types of  $\beta$ -SiAlON ( $\text{Si}_{6-z}\text{Al}_z\text{O}_z\text{N}_{8-z}$ ) powder were prepared by the carbothermal reduction and simultaneous nitridation of ultrafine powders in the  $\text{Al}_2\text{O}_3$ - $\text{SiO}_2$  system. The ultrafine starting oxide powders, prepared using the vapour-phase reaction technique, were mixed with carbon powder and heated at 1400 °C for 1 h under flowing nitrogen to form  $\beta$ -SiAlON and followed by heating at 570 °C for 1 h in air to remove residual carbon. The resulting powders contained only  $\beta$ -SiAlON with  $z$  values of 1.63, 2.05, and 2.99. The relative density (bulk density/true density) of  $\beta$ -SiAlON compacts pressureless sintered at 1800 °C for 1 h under flowing nitrogen increased with  $z$  and reached 89.9% at  $z = 2.99$ . When the  $\beta$ -SiAlON compact with  $z = 2.99$  was hot pressed at 1800 °C for 1 h under flowing nitrogen, a maximum relative density of 93.6% was achieved. Although this hot pressed compact contained a small amount of 15R-SiAlON in addition to  $\beta$ -SiAlON, it possessed a small average grain size (typically 0.5  $\mu\text{m}$  diameter) and high Vickers hardness (19.2 GPa).  
 © 2001 Kluwer Academic Publishers

## 1. Introduction

The mechanical and physical properties of silicon nitride ( $\text{Si}_3\text{N}_4$ ) and its related SiAlON family (chemical formula:  $\text{Si}_{6-z}\text{Al}_z\text{O}_z\text{N}_{8-z}$ ) of ceramics [1–15] are known to depend greatly upon such factors as the characteristics of the starting powder [4, 5, 11, 13], sintering conditions [6], additives [12], phase composition [2], and microstructure [14]. Several different techniques exist for the preparation of  $\text{Si}_3\text{N}_4$  powder, i.e., (i) direct nitridation of silicon [7, 10], (ii) carbothermal reduction of silica ( $\text{SiO}_2$ ) in a nitrogen atmosphere [3], (iii) vapour-phase reaction between ammonia ( $\text{NH}_3$ ) and silicon tetrachloride ( $\text{SiCl}_4$ ) or silane ( $\text{SiH}_4$ ) [8], and (iv) pyrolysis of an organometallic polymer in the presence of  $\text{NH}_3$  [9]. Although similar techniques also exist for the preparation of  $\beta$ -SiAlON powder, most work has focused on solid state reactions using metal oxides and nitrides, i.e.,  $\text{Si}_3\text{N}_4$ ,  $\text{SiO}_2$ ,  $\text{AlN}$  and  $\text{Al}_2\text{O}_3$ . From the viewpoint of mechanical properties at elevated temperature it is preferable to reduce the use of sintering aids (e.g., rare earth oxides) to a minimum. Therefore  $\beta$ -SiAlON powder with submicrometre-sized particles has an advantage over most powders, whose size is typically  $>1 \mu\text{m}$ , as densification may be achieved without the addition of sintering aids such as yttrium oxide ( $\text{Y}_2\text{O}_3$ ) and/or at a lower sintering temperature [15].

Among the preparation methods for  $\beta$ -SiAlON powder, therefore, the carbothermal reduction and simultaneous nitridation (CRSN) technique is useful as it results in formation of submicrometre-sized  $\beta$ -SiAlON powder. Starting powders investigated in the  $\text{Al}_2\text{O}_3$ - $\text{SiO}_2$  system for the CRSN technique have included: (i) mixtures of  $\text{SiO}_2$ ,  $\text{Al}_2\text{O}_3$ , and C powders [16, 17], (ii) kaolinite ( $2\text{SiO}_2 \cdot \text{Al}_2\text{O}_3 \cdot 2\text{H}_2\text{O}$ ) [18], (iii) mixtures of  $\text{SiO}_2$ ,  $\text{Al}_2\text{O}_3 \cdot 2\text{H}_2\text{O}$  and C powders [19], and (iv) alkoxides obtained by the hydrolysis of silicon tetraethoxide and aluminium isopropoxide [20, 21]. Several of the present authors have prepared such a candidate material (high purity mullite ( $3\text{Al}_2\text{O}_3 \cdot 2\text{SiO}_2$ ) powder with average diameter of  $\sim 0.05 \mu\text{m}$ ) using the chemical vapour deposition (CVD) technique and aluminium chloride ( $\text{AlCl}_3$ ),  $\text{SiCl}_4$ , and oxygen [22, 23]. The  $\text{Al}_2\text{O}_3/\text{SiO}_2$  ratio of this ultrafine powder could be controlled through varying the experimental conditions (e.g., sublimation rates of the starting metal chlorides, flow rate of the carrier gas, reaction temperature, etc.). The preparation of ultrafine  $\beta$ -SiAlON powders with various  $z$  values is therefore made possible by the CRSN of such ultrafine powders in the  $\text{SiO}_2$ - $\text{Al}_2\text{O}_3$  system that might be expected to react readily with fine C powder. The present work is thus concerned with: (i) determination of conditions necessary for the preparation

\* Author to whom all correspondence should be addressed.

of  $\beta$ -SiAlON powders using the CRSN technique, (ii) characterisation of the resulting powders, and (iii) fabrication of dense ceramics using these powders.

## 2. Experimental procedure

The  $\beta$ -SiAlON powders investigated in this work were prepared using powders in the  $\text{Al}_2\text{O}_3$ - $\text{SiO}_2$  system and active carbon powder (Wako Pure Chemical Ind. Ltd., Osaka Japan). Preparation details of the powders in the  $\text{Al}_2\text{O}_3$ - $\text{SiO}_2$  system have been given elsewhere [22] but are briefly repeated here. The starting  $\text{AlCl}_3$  powder (Aldrich Chemical Company Inc.; 99.9% purity) and  $\text{SiCl}_4$  solution (Soekawa Chemicals; 99.999% purity) were vapourised at 200 °C and 30–40 °C, respectively, and introduced into the upper side of a heating zone (mullite tube; length 1000 mm, inner diameter 60 mm) using Ar gas as a carrier whilst oxygen was simultaneously introduced. The temperature of the upper part of the heating zone was varied between 750 °C and 900 °C whilst that of the lower part was kept constant at 400 °C. The oxygen and argon flow rates were 1.0 and 0.3  $\text{dm}^3\cdot\text{min}^{-1}$ , respectively, with the  $\text{AlCl}_3$  and  $\text{SiCl}_4$  vapour reacting with oxygen to form a powder in the  $\text{Al}_2\text{O}_3$ - $\text{SiO}_2$  system. The powder was collected in a test tube-type filter whilst chloride vapour resulting from the reaction was neutralised using concentrated sodium hydroxide (NaOH) solution. The powders were calcined at 200 °C for 30 min in order to remove residual chlorides.

The powders in the  $\text{Al}_2\text{O}_3$ - $\text{SiO}_2$  system were then mixed together with activated carbon powder in the presence of acetone using an alumina mortar and pestle. The amount of carbon was three times as large as that calculated for full conversion of the powder to  $\beta$ -SiAlON. Carbothermal reduction and simultaneously nitridation was achieved using a flowing nitrogen atmosphere (2.0  $\text{dm}^3\cdot\text{min}^{-1}$ ) for 90 min at 1300–1450 °C and followed by a heat treatment in air at 570 °C for 1 h in order to remove any residual carbon. Properties of a commercially available  $\beta$ -SiAlON powder (UBE-SN-SZ3, Ube Industries Ltd., Ube, Japan) were also examined for use as a reference material. The Si/Al ratio and  $z$  value of the commercial  $\beta$ -SiAlON powder were found to be 0.98 and 3.03, respectively, whilst the specific surface area (SSA) was 3.8  $\text{m}^2\cdot\text{g}^{-1}$ .

Sintered compacts were fabricated from the powders using either pressureless sintering or hot pressing techniques. For the pressureless sintering technique, approximately 0.3 g of powder was isostatically pressed at 100 MPa to form a disk with diameter of 10 mm and thickness of  $\sim 2$  mm. The disk was then embedded in an equimolar mixture of  $\text{Si}_3\text{N}_4$  and  $\text{SiO}_2$  powder, in order to prevent any thermal decomposition of the expected  $\beta$ -SiAlON [21], and heated from room temperature to 1100 °C at a rate of 30 °C $\cdot\text{min}^{-1}$  and from 1100 °C to 1800 °C at 10 °C $\cdot\text{min}^{-1}$ . The firing time at each temperature was fixed to be 1 h whilst resulting sintered compacts were furnace cooled. For the hot-pressing technique, approximately 1.0 g of powder was first uniaxially pressed at 30 MPa in a steel die and then isostatically pressed at 100 MPa in order to form a disk with diameter of 20 mm and thickness of  $\sim 2$  mm. The

compact was heated in a graphite die from room temperature up to 1100 °C at a rate of 30 °C $\cdot\text{min}^{-1}$  and from 1100 °C to 1800 °C at 10 °C $\cdot\text{min}^{-1}$  under a pressure of 31 MPa and held for 1 h in a flowing nitrogen atmosphere. The relative density of sintered compacts was calculated by dividing the bulk density by true density. The bulk density was measured on the basis of mass and dimensions whilst the true density was measured using the Archimedes method at 30.0 °C (immersion liquid; ethanol) after the sintered compact was pulverized using an alumina mortar and pestle.

Crystalline phases of the resulting powder and sintered compacts were determined using an X-ray diffractometer (XRD) with Cu  $K_\alpha$  radiation (40 kV, 25 mA; Model RAD-IIA, Rigaku, Tokyo, Japan) and referenced using Joint Committee on Powder Diffraction Standards (JCPDS) cards. The specific surface area (SSA) of the powder was determined using a Brunauer-Emmett-Teller (BET) technique with nitrogen as an adsorption gas. Particle shapes and morphologies were observed using a transmission electron microscope (TEM) (accelerating voltage, 300 kV; Model H-9000, Hitachi, Tokyo, Japan) whilst microstructures of the sintered compacts were investigated using a scanning electron microscope (SEM) (accelerating voltage, 5 kV; Model S-4500, Hitachi, Tokyo, Japan) after the specimen surface was first etched using concentrated HF and then coated with Pt/Pd in order to reduce charging effects. The amounts of aluminium and silicon in the powder were determined using a SEM fitted with energy dispersive X-ray microanalysis (EDX) (Model EMAX-5770, Horiba, Kyoto, Japan) whilst the amounts of oxygen and nitrogen were determined using a determinator (Model TC-136, LECO, St. Joseph, MI, USA). Vickers hardness,  $H_V$ , was evaluated for the sintered compacts using an indentation load and time of 1 kg and 15 s, respectively (Akashi, Model MVK-E, Tokyo, Japan).

## 3. Results and discussion

### 3.1. Properties of powder in the $\text{Al}_2\text{O}_3$ - $\text{SiO}_2$ system prepared by the CVD technique

Prior to performing the CRSN procedure, properties of the powders in the  $\text{Al}_2\text{O}_3$ - $\text{SiO}_2$  system were examined with analytical results of the compositions being shown in Table I. It can be seen that the powder SSA decreased with decreasing Al/Si ratio. For example, the SSA of the powder with an Al/Si ratio of 1.25 was 45.6  $\text{m}^2\cdot\text{g}^{-1}$ , compared to a SSA of 121.8  $\text{m}^2\cdot\text{g}^{-1}$  for the Al/Si ratio of 2.75. The chlorine content for all powders was found to be on the order of 1 mol%.

Crystalline phases of the resulting powders were examined using XRD with results being presented in

TABLE I Chemical composition of the starting oxide powders prepared using the CVD technique

Sample No.	Si mol%	Al mol%	Cl mol%	Si Al	SSA $\text{m}^2\cdot\text{g}^{-1}$
1	19.87	15.89	0.66	1.25	45.6
2	24.22	9.88	1.37	2.45	58.4
3	25.29	9.21	0.97	2.75	121.8

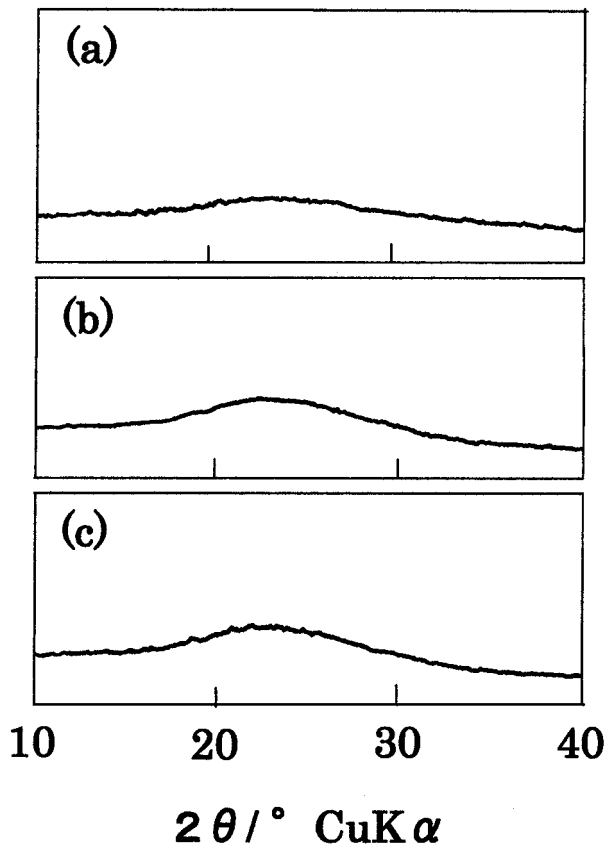
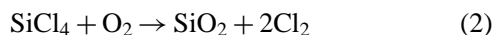
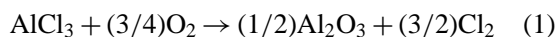


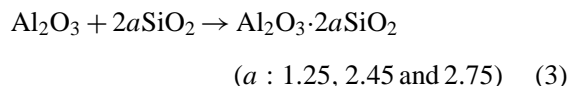
Figure 1 X-ray diffraction patterns of the starting oxide powders prepared using the CVD technique: (a) Sample 1, (b) Sample 2, and (c) Sample 3.

Fig. 1. The lack of any distinct reflections showed these powders to be essentially amorphous.

The reaction processes of the metal chlorides to metal oxides may be expressed as follows:



Each mole of  $\text{Al}_2\text{O}_3$  then reacts instantaneously with some amount of  $\text{SiO}_2$  to form amorphous material in the  $\text{Al}_2\text{O}_3\text{-SiO}_2$  system such that:



The starting powders in the present case possessed high SSA (i.e., ultrafine particles) together with low chlorine content. The decrease of SSA with Al content in the powder may be attributed to the difference in reactivity of oxygen between  $\text{AlCl}_3$  and  $\text{SiCl}_4$ , with details being discussed later, together with the data on particle morphology. On the other hand, the generally low chlorine content in these powders demonstrates that oxidation of these metal chlorides occurs effectively with the almost total elimination of chlorine from the system.

Particle morphologies of the resulting powders were observed using TEM with a typical micrograph of Sample 1 being presented in Fig. 2. The particles exhibited spherical shell structures with diameters of typically less than  $\sim 0.1 \mu\text{m}$  whilst the inner core of

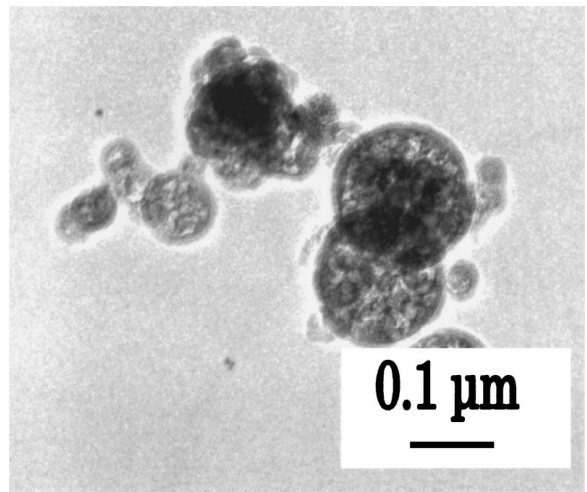


Figure 2 Typical TEM micrograph of a starting oxide powder (Sample 1) prepared using the CVD technique.

each particle consisted of a highly porous network surrounded by a thin and denser shell. Such a highly porous network would explain the high SSA value ( $45.6 \text{ m}^2 \cdot \text{g}^{-1}$ ) obtained for this powder.

The particle formation route using the vapour phase reaction may be divided into two stages, i.e., homogeneous nucleation and growth [24]. Since the reactivity of  $\text{AlCl}_3$  with oxygen may be appreciably greater than that of  $\text{SiCl}_4$  with oxygen [24], the nucleation of  $\text{Al}_2\text{O}_3$  would be thought to occur more readily than that of  $\text{SiO}_2$ . Such a hypothesis is also supported by the fact that the powder SSA decreased with Al content. Although the particles consist of a highly porous network surrounded by a thin and denser shell, the chemical composition of the outer shell is believed to be almost the same as that of the inner core as a result of the homogeneous nucleation and growth of the particles.

### 3.2. Properties of $\beta$ -SiAlON powders prepared by the CRSN technique

The optimum conditions for the preparation of  $\beta$ -SiAlON using the CRSN technique were investigated for the oxide powders prepared by the CVD technique in the previous section. First of all, the effect of temperature on phase changes during CRSN was examined using XRD with typical XRD patterns for Sample 1 being shown in Fig. 3. For a reaction temperature of  $1300^\circ\text{C}$ ,  $\beta$ -SiAlON ( $z = 3$ ;  $\text{Si}_3\text{Al}_3\text{O}_3\text{N}_5$ ) [25],  $\alpha$ - $\text{Si}_3\text{N}_4$  [26], X-phase, [27] and mullite [28] were found to be present in the powder. The formation routes of X-phase by CRSN have been previously examined by Zheng and Forslund [17], who suggested that X-phase may form as an intermediate phase from a mixture of  $\text{SiO}_2$  and  $\text{Al}_2\text{O}_3$  powder but not from kaolin. It would therefore appear to be the case that X-phase is an intermediate phase during the formation of  $\beta$ -SiAlON from mullite. For a reaction temperature of  $1350^\circ\text{C}$ ,  $\beta$ -SiAlON together with a small amount of  $\alpha$ - $\text{Si}_3\text{N}_4$  were found to be present in the powder whilst reaction temperatures of  $1400^\circ\text{C}$  and  $1450^\circ\text{C}$  showed only  $\beta$ -SiAlON to be present. From this data it may be concluded that

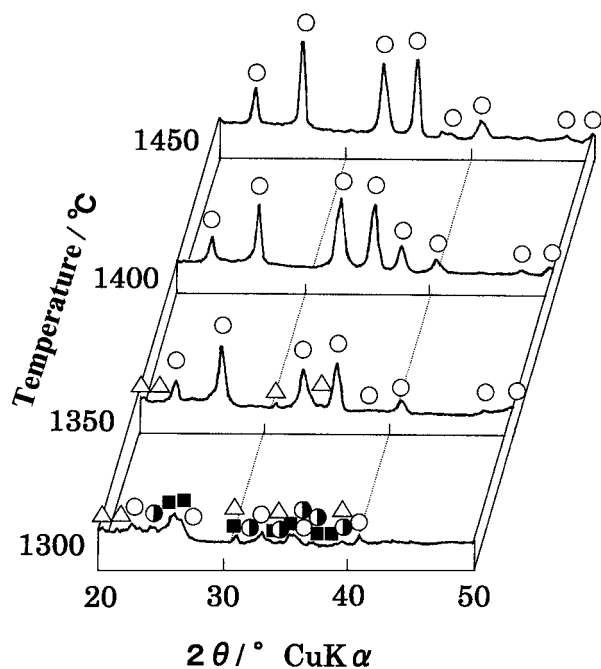


Figure 3 Typical XRD patterns following carbothermal and simultaneous nitridation processing of Sample 1. Heating time: 1 h. ○:  $\beta$ -SiAlON, ○: X-phase,  $\Delta$ :  $\alpha$ -Si<sub>3</sub>N<sub>4</sub>, ■: Mullite.

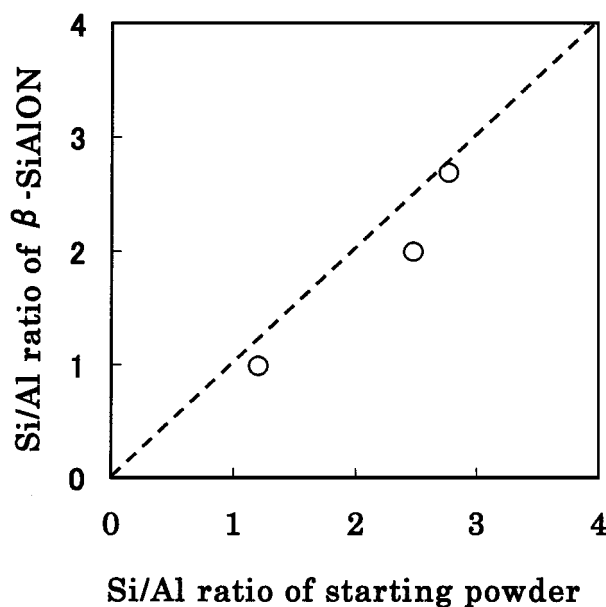


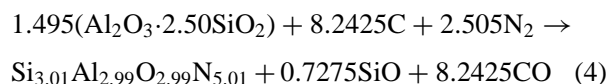
Figure 4 Relationship between the Si/Al ratio for the starting powder and  $\beta$ -SiAlON powder.

1400 °C is the minimum temperature required for complete conversion of the starting oxide powders into  $\beta$ -SiAlON. It is noteworthy that CRSN of the present powders may be carried out at a temperature as low as 1400 °C whereas kaolinite-derived powder [18] and alkoxy-derived powder [21] are nitrided at 1500 °C and 1430 °C, respectively. Based upon the above information, the heating temperature and time for the preparation of  $\beta$ -SiAlON powder were fixed to be 1400 °C and 1 h, respectively.

Analytical data for the resulting  $\beta$ -SiAlON powders were plotted against those of the starting powders in the Al<sub>2</sub>O<sub>3</sub>-SiO<sub>2</sub> system and presented in Fig. 4. It should be noted that the resulting  $\beta$ -SiAlON powders were fur-

ther heat-treated in air at 570 °C for 1 h in order to remove any residual carbon. Si/Al ratios of the  $\beta$ -SiAlON powders were somewhat lower compared to those of the starting powders in the Al<sub>2</sub>O<sub>3</sub>-SiO<sub>2</sub> system with Si/Al ratios being in the range 1.01–2.68. Calculated  $z$  values for these  $\beta$ -SiAlON powders were found to be 1.63, 2.05, and 2.99.

As stated above, the Si/Al ratios of  $\beta$ -SiAlON powders were lower than those of their respective starting Al<sub>2</sub>O<sub>3</sub>-SiO<sub>2</sub> powders and this may be explained in terms of the vapourization of Si to form SiO during the CRSN procedure [17–19, 21]. As the Si/Al ratio of Sample 1 was reduced from 1.25 to 1.01 by the CRSN process, the stoichiometric reaction route may be expressed as follows:



In order to confirm whether or not the stoichiometric amounts of oxygen and nitrogen were present in the  $\beta$ -SiAlON shown in Equation 4, these amounts were determined quantitatively. On the basis of this data, the chemical composition of Sample 1 was determined to be Si<sub>3.03</sub>Al<sub>3.00</sub>O<sub>3.93</sub>N<sub>4.04</sub>. Comparing this composition with the theoretical composition shown in Equation 4, the present  $\beta$ -SiAlON has a larger amount of oxygen and smaller amount of nitrogen, which suggests that CRSN requires a long time to complete the procedure, regardless of the relatively high SSA value (45.6 m<sup>2</sup>·g<sup>-1</sup>) of the starting powder in the Al<sub>2</sub>O<sub>3</sub>-SiO<sub>2</sub> system. The reason for this anomaly may be that the outer spherical shell structure retards the CNRS reaction of the inner porous structure.

A typical TEM micrograph showing the morphology of the  $\beta$ -SiAlON powder (Sample 1) has been given in Fig. 5. It can be seen that these  $\beta$ -SiAlON particles possessed equiaxed structures with diameters of ~0.05  $\mu$ m and a fully dense interior, in contrast to the corresponding particles in the Al<sub>2</sub>O<sub>3</sub>-SiO<sub>2</sub> system which exhibited a highly porous interior (Fig. 3). The SSA value for this  $\beta$ -SiAlON powder was 24.8 m<sup>2</sup>·g<sup>-1</sup> and still relatively high despite being reduced during the CRSN process.

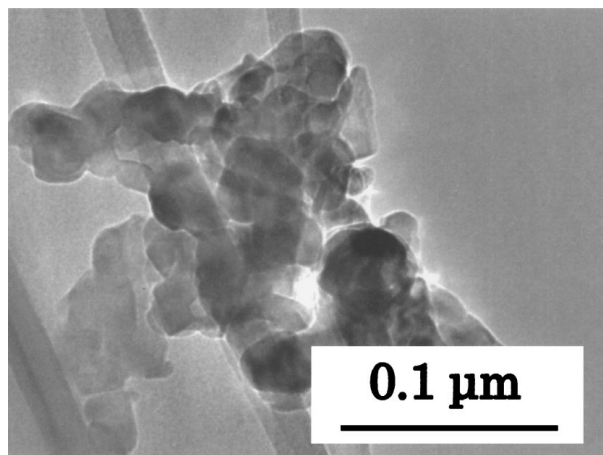


Figure 5 Typical TEM micrograph of  $\beta$ -SiAlON powder with  $z = 2.99$ .

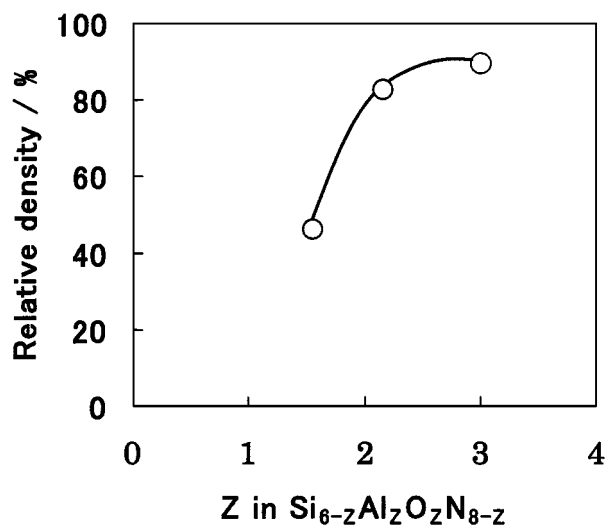


Figure 6 Relationship between  $z$  value and relative density for  $\beta$ -SiAlON compacts fired at 1800 °C for 1 h under a flowing nitrogen atmosphere.

### 3.3. Sinterability of the $\beta$ -SiAlON powders

The effect of  $z$  (in the formula  $\text{Si}_{6-z}\text{Al}_z\text{O}_z\text{N}_{8-z}$ ) on relative density for  $\beta$ -SiAlON ceramics fabricated using the pressureless sintering technique has been shown in Fig. 6. Although the relative density of  $\beta$ -SiAlON compacts pressureless sintered at 1800°C for 1 h was only ~45% for the case of  $z = 1.63$ , this increased to ~80% for  $z = 2.05$ , and 89.9% for the case of  $z = 2.99$ .

For the present pressureless sintering conditions (1800 °, 1 h, flowing nitrogen), maximum relative density (89.9%) of the  $\beta$ -SiAlON ceramic with  $z = 2.99$  was noted to be approximately 15% greater compared to that of a  $\beta$ -SiAlON ceramic fabricated using the commercially available powder (75.4%). Sinterability of the present  $\beta$ -SiAlON powder with  $z = 2.99$  may be enhanced not only by the high SSA and/or small particle size but also as a result of the higher Al content (i.e., higher  $z$  value). The effect of  $z$  value on the sinterability of  $\beta$ -SiAlON has been examined by Mitomo *et al.* [29], who demonstrated that sinterability is enhanced for the case of  $z \geq 2$ . Such a conclusion is also in accordance with the present data.

Since the  $\beta$ -SiAlON powder with  $z = 2.99$  showed excellent sinterability, the densification processes of the present and commercially available powder compacts were examined with results being presented in Fig. 7. For a firing temperature of 1500 °C, there was little difference in relative density between the present and commercially available powders. However, relative density of the present  $\beta$ -SiAlON compacts became larger compared to those of the commercially available powder with increasing firing temperature. At a firing temperature of 1800 °C, relative density of the  $\beta$ -SiAlON ceramic with  $z = 3.03$  fabricated using commercially available powder was limited to approximately 75% whilst that of the present  $\beta$ -SiAlON ceramic with  $z = 2.99$  attained 89.9%.

SEM micrographs of  $\beta$ -SiAlON compacts pressureless sintered using the present powder (Sample 1) and commercially available powder have been shown in Fig. 8a and b, respectively, together with their grain

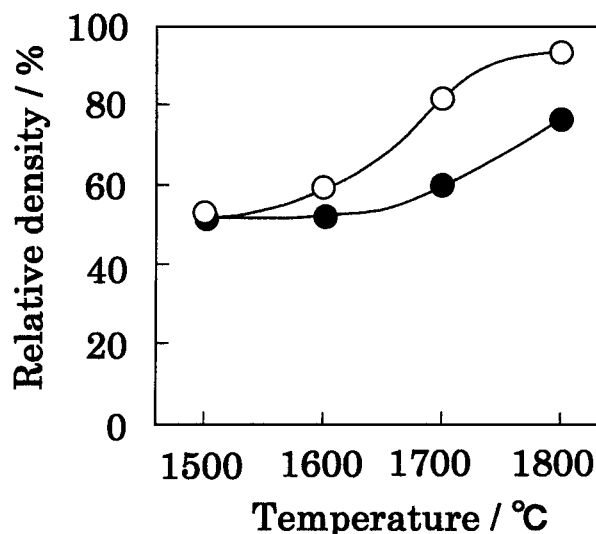


Figure 7 Relationship between relative density and firing temperature for  $\beta$ -SiAlON compacts. Firing time: 1 h. ○:  $\beta$ -SiAlON compact with  $z = 2.99$  fabricated using the present powder, ●:  $\beta$ -SiAlON compact with  $z = 3.03$  fabricated using the commercially available powder.

size distributions and median grain sizes. Although both pressureless sintered compacts were composed of equiaxed grains, a significant difference in grain diameter was apparent between them. The  $\beta$ -SiAlON compact pressureless sintered using the present powder possessed equiaxed grains with diameters of  $<0.3 \mu\text{m}$  and a median grain diameter estimated to be  $0.09 \mu\text{m}$  (Fig. 8a and a'). However, the  $\beta$ -SiAlON compact pressureless sintered using commercially available powder possessed equiaxed grains with diameters of  $<3 \mu\text{m}$  and a median diameter estimated to be  $1.34 \mu\text{m}$  (Fig. 8b and b').

The median grain size of the  $\beta$ -SiAlON compact pressureless sintered using the present powder was thus a factor of 15 smaller compared to that of pressureless sintered compacts using the commercially available powder. Since the SSAs of the present and commercially available powders were  $24.8 \text{ m}^2 \cdot \text{g}^{-1}$  and  $3.8 \text{ m}^2 \cdot \text{g}^{-1}$ , respectively, powders prepared in this work show the potential to fabricate dense  $\beta$ -SiAlON ceramics with nanosized grain structures ( $<100 \text{ nm}$  diameter).

As the maximum relative density of the pressureless sintered  $\beta$ -SiAlON compact with  $z = 2.99$  was 89.9%, and thus could not exceed 90%, hot pressing was conducted in order to promote further densification. The hot pressing temperature and time were chosen to be 1800 °C and 1 h, respectively, and thus the same as those for pressureless sintering. Relative density of the hot pressed compact fabricated using the present powder compacts was determined to be 93.6%.

In addition, XRD patterns for the hot pressed and pressureless sintered compacts with  $z = 2.99$  have been given in Fig. 9. The pressureless sintered compact was found to contain only  $\beta$ -SiAlON (Fig. 9a) whereas the hot pressed compact contained  $\beta$ -SiAlON together with a smaller amount of 15R-SiAlON [30] (Fig. 9b).

The 15R-SiAlON formed in the hot pressed compact was attributed to partial decomposition of  $\beta$ -SiAlON due to the elimination of some components during hot

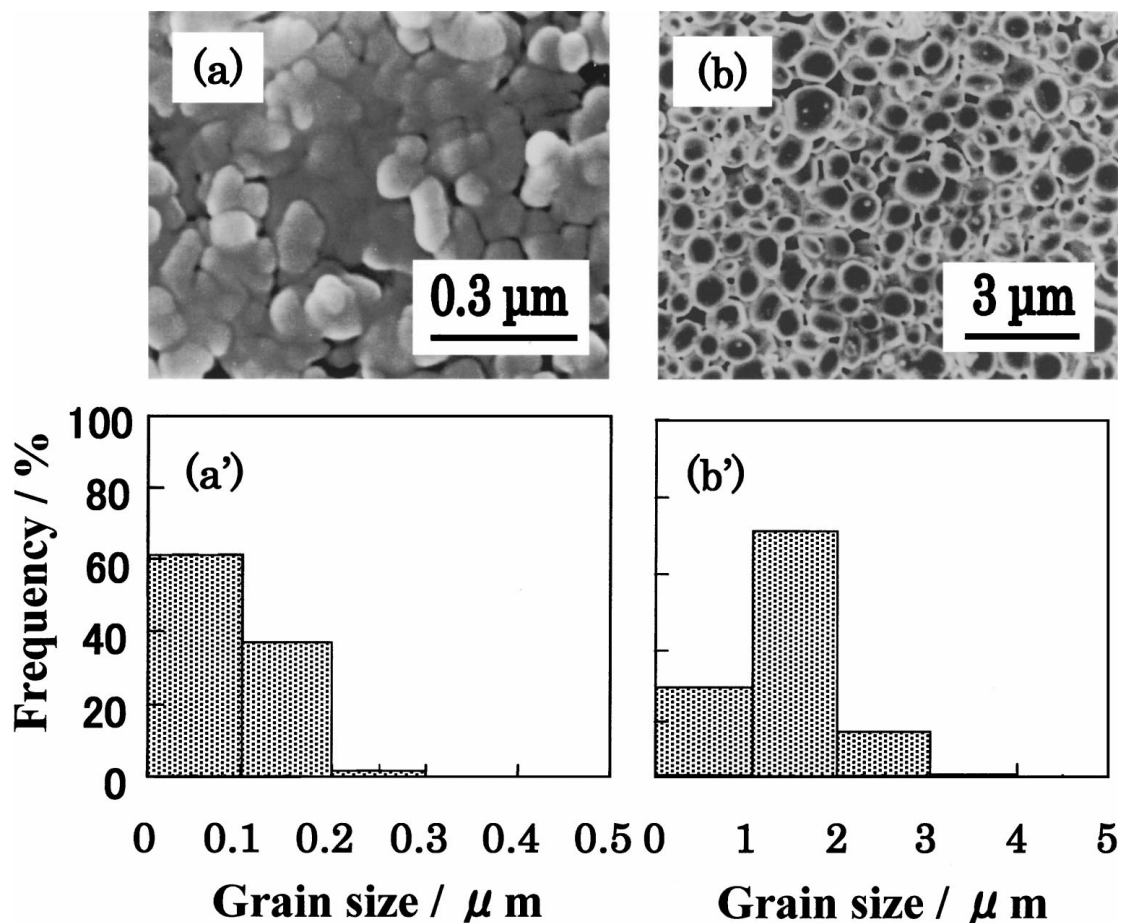


Figure 8 Typical SEM micrographs and grain-size distributions for  $\beta$ -SiAlON compacts pressureless sintered at 1800 °C for 1 h. Note that the surfaces of these compacts were etched using concentrated HF solution. (a) and (a'):  $\beta$ -SiAlON compact with  $z = 2.99$  fabricated using the present powder (median grain size: 0.09  $\mu\text{m}$ ); (b) and (b'):  $\beta$ -SiAlON compact with  $z = 3.03$  fabricated using commercially available powder (median grain size: 1.34  $\mu\text{m}$ ).

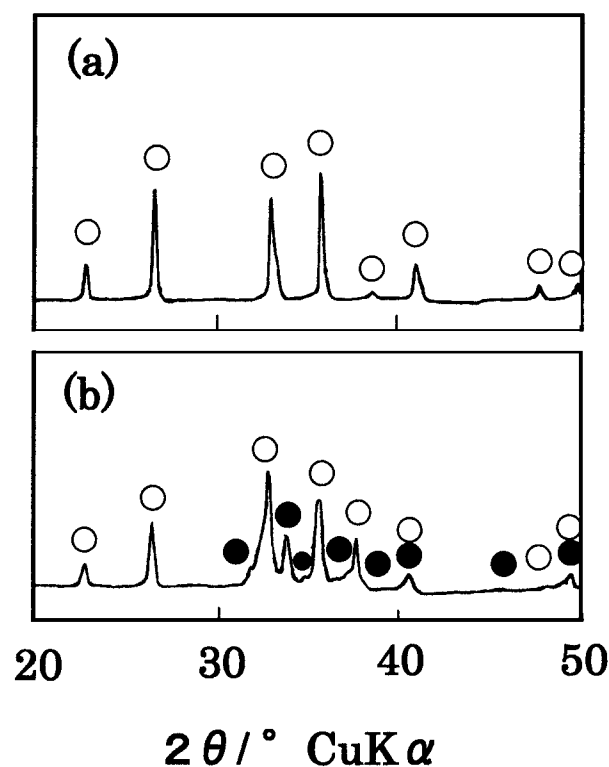


Figure 9 Typical XRD patterns for the present compacts with  $z = 2.99$ : (a) pressureless sintered, and (b) hot-pressed at 1800 °C for 1 h.  $\circ$ :  $\beta$ -SiAlON,  $\bullet$ : 15R-SiAlON.

pressing [29]. Note that no 15R-SiAlON was detected in the pressureless sintering case as the  $\beta$ -SiAlON compact was fired whilst embedded in an equimolar mixture of  $\text{Si}_3\text{N}_4$  and  $\text{SiO}_2$  powder in order to prevent such thermal decomposition [29].

A SEM micrograph showing the etched surface of a hot pressed compact using the present powder (Sample 1) has been presented in Fig. 10. This compact was

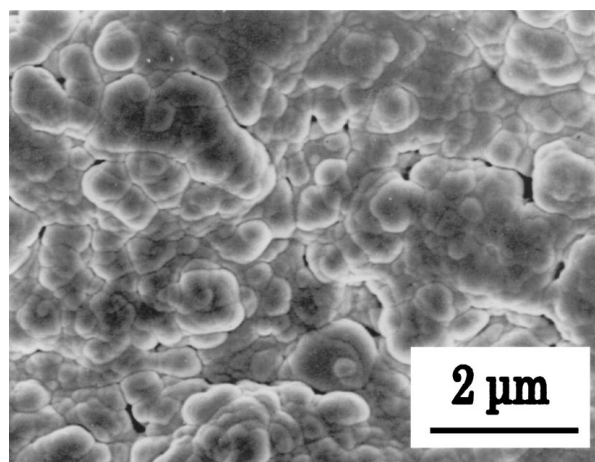


Figure 10 Typical SEM micrograph of the compact with  $z = 2.99$  hot-pressed at 1800 °C for 1 h. Note that the surface of this compact was etched using concentrated HF solution.

seen to contain grains with a mean diameter of typically  $0.5\ \mu\text{m}$ .

In general,  $\beta$ -SiAlON ceramics have been fabricated by the reaction sintering of powder mixtures in the  $\text{Si}_3\text{N}_4$ ,  $\text{SiO}_2$ ,  $\text{AlN}$ , and  $\text{Al}_2\text{O}_3$  systems. In this case, “transient” liquids that form during sintering promote densification, chiefly due to the rearrangement of grains. In the present paper, however, the amount of “transient” liquid phase would appear to be negligible in comparison with the case of reaction sintering. This assumption may be supported by the fact that the present grain size (typically  $0.5\ \mu\text{m}$ ) was smaller than that formed by reaction sintering [31]. The present sintering therefore appears to proceed by mass transfer due to the high SSA and excess amount of oxygen over stoichiometry.

Vickers hardness was also measured for the hot pressed compact and found to be 19.2 GPa and thus higher or equal to that of other SiAlON ceramics manufactured using a variety of methods [32–34]. Such a high Vickers hardness was attributed to both the small grain diameter (typically  $0.5\ \mu\text{m}$ ) and also the small amount of glassy phase thought to be present at grain boundaries of a sintered SiAlON compact without the use of additives. The fracture toughness of hot pressed compacts was not measured in the present work. However, the fracture toughness values of (i)  $\beta$ -SiAlON ceramic fabricated by the CRSN of alkoxide-derived  $\text{SiO}_2$ - $\text{Al}_2\text{O}_3$  powder and (ii)  $\beta$ -SiAlON ceramic fabricated using  $\text{Si}_3\text{N}_4$ ,  $\text{AlN}$ , and  $\text{Al}_2\text{O}_3$  have been measured by Mitomo *et al.* [35], who pointed out that no marked difference in fracture toughness was observed between these ceramics, regardless of any increase in Vickers hardness.

As mentioned above, sintering does not appear to proceed by liquid phase sintering but instead by solid state sintering. Since grain growth may be inhibited using the present  $\beta$ -SiAlON powder, the mechanical strength (e.g., flexural strength, compressive strength, etc.) might be expected to be higher in comparison with the case of the reaction sintering technique. The relationship between mechanical strength and microstructure for these sintered compacts will be reported at a later date.

#### 4. Conclusions

Three types of  $\beta$ -SiAlON ( $\text{Si}_{6-z}\text{Al}_z\text{O}_z\text{N}_{8-z}$ ) powder were prepared by the carbothermal reduction and simultaneous nitridation of ultrafine powders in the  $\text{Al}_2\text{O}_3$ - $\text{SiO}_2$  system. The densification and microstructures of the  $\beta$ -SiAlON ceramics were examined with results being summarised as follows:

(1) The ultrafine starting powders in the  $\text{Al}_2\text{O}_3$ - $\text{SiO}_2$  system, prepared by the vapour-phase reaction technique, were mixed with carbon powder and heated in a flowing nitrogen atmosphere ( $1400\ ^\circ\text{C}$  for 1 h) followed by heating in air ( $570\ ^\circ\text{C}$  for 1 h) to remove residual carbon. The resulting powders contained only  $\beta$ -SiAlON whose  $z$  values were 1.63, 2.05 and 2.99.

(2) The relative density (bulk density/true density) of the  $\beta$ -SiAlON compacts pressureless sintered at

$1800\ ^\circ\text{C}$  for 1 h under a flowing nitrogen atmosphere increased with  $z$  in the formula  $\text{Si}_{6-z}\text{Al}_z\text{O}_z\text{N}_{8-z}$  to reach 89.9% at  $z = 2.99$ . This sintered compact was composed of equiaxed grains with a mean diameter of  $0.09\ \mu\text{m}$ .

(3) When the  $\beta$ -SiAlON compact with  $z = 2.99$  was hot pressed at  $1800\ ^\circ\text{C}$  for 1 h under a flowing nitrogen atmosphere, relative density attained 93.6% whilst the main phases were determined to be  $\beta$ -SiAlON and 15R-SiAlON. This sintered compact possessed a small grain size (typically  $0.5\ \mu\text{m}$  diameter) and high Vickers hardness (19.2 GPa).

#### Acknowledgements

The authors wish to express their thanks to Professor Dr. Y. Toda and Dr. K. Hashimoto of Chiba Institute of Technology for taking the TEM micrographs.

#### References

1. M. L. TORTI, in “Treatise on Materials Science and Technology, Vol. 29,” edited by J. B. Wachtman (Academic Press, London, UK, 1989) p. 161.
2. E. TANI, S. UMEBAYASHI, K. OKUZONO, K. KISHI and K. KOBAYASHI, *Yogyo-Kyokai-Shi*, **93** (1985) 370.
3. H. HOFMAN, U. VOGT, A. KERBER and F. VAN DIJEN, in *Mat. Res. Soc. Symp. Proc.* (Materials Research Society, USA, 1993) Vol. 287, p. 105.
4. G. WOETTING, H. FEUER and E. GUDEL, in *Mat. Res. Soc. Symp. Proc.* (Materials Research Society, USA, 1993) Vol. 287, p. 133.
5. A. BELLOSI and G. N. BABINI, in “Key Engineering Materials, Vol. 161–163” (Trans Tech Publications, Switzerland, 1999) p. 203.
6. H. MANDAL, D. P. THOMPSON and T. EKSTÖM, in “Third Euro-Ceramics,” edited by P. Durán and J. F. Fernández (Faenza Editrice Ibérica S.L., Spain, 1993) p. 385.
7. T. ITOH, *J. Mater. Sci. Lett.* **9** (1990) 19.
8. B. W. JONG, G. J. SLAVENS and D. E. TRAUULT, *J. Mater. Sci.* **27** (1992) 6086.
9. W. R. SCHMIDT, V. SUKUMAR, W. J. HURLEY, R. GARCIA, R. H. DOREMUS, L. V. INTERRANTE and G. M. RENLUND, *J. Amer. Ceram. Soc.* **73** (1990) 2412.
10. D. L. SEGAL, *Br. Ceram. Trans. J.* **85** (1996) 184.
11. G. WOTTING and G. ZIEGLER, *Powder Metall. Int.* **18** (1986) 25.
12. S. HAMPSHIRE, M. J. POMEROY and B. SARUHAN, in “High Tech Ceramics,” edited by P. Vincenzini (Elsevier Science Publishers B.V., Amsterdam, The Netherlands, 1987) p. 941.
13. A. KATO, K. SARUGAKU and S. SAMESHIMA, in “High Tech Ceramics,” edited by P. Vincenzini (Elsevier Science Publishers B.V., Amsterdam, The Netherlands, 1987) p. 911.
14. G. RIEDEL and H. KRÜNER, in “Third Euro-Ceramics, Vol. 3,” edited by P. Durán and J. F. Fernández (Faenza Editrice Ibérica S.L., Spain, 1993) p. 453.
15. K. H. JACK, *J. Mater. Sci.* **11** (1976) 1135.
16. J. W. T. VAN RUTTEN, R. A. TERPSTRA, J. C. T. VAN DER HEIJDE, H. T. HINTZEN and R. METSELAAR, *J. Europ. Ceram. Soc.* **15** (1995) 599.
17. J. ZHENG and B. FORSLUND, *ibid.* **19** (1999) 175.
18. H. YOSHIMATSU, M. MITOMO, H. MIHASHI, B. OHMORI and T. YABUKI, *Yogyo-Kyokai-Shi*, **91** (1983) 442.
19. H. YOSHIMATSU, T. YABUKI and H. MIHASHI, *ibid.* **95** (1987) 590.
20. M. HOCH and K. M. NAIR, *J. Amer. Ceram. Soc.* **58** (1979) 191.
21. M. MITOMO, T. SHIOGAI, H. YOSHIMATSU and Y. KITAMI, *Yogyo-Kyokai-Shi*, **93** (1985) 364.
22. K. ITATANI, T. KUBOZONO, F. S. HOWELL, A. KISHIOKA and M. KINOSHITA, *J. Mater. Sci.* **30** (1995) 1158.

23. *Idem., ibid.* **30** (1995) 1196.
24. Y. SUYAMA and A. KATO, *J. Amer. Ceram. Soc.* **59** (1976) 146.
25. Powder diffraction file card No. 36-1333 (JCPDS-International Center for Diffraction Data, Swarthmore, PA).
26. Powder diffraction file card No. 41-360 (JCPDS-International Center for Diffraction Data, Swarthmore, PA).
27. Powder diffraction file card No. 35-23 (JCPDS-International Center for Diffraction Data, Swarthmore, PA).
28. Powder diffraction file card No. 15-776 (JCPDS-International Center for Diffraction Data, Swarthmore, PA).
29. M. MITOMO, N. KURAMOTO and Y. YAJIMA, *Yogyo-Kyokai-Shi.* **88** (1980) 49.
30. Powder diffraction file card No. 42-160 (JCPDS-International Center for Diffraction Data, Swarthmore, PA).
31. M. MITOMO, N. KURAMOTO, Y. INOMATA and M. TSUTSUMI, *Yogyo-Kyokai-Shi.* **88** (1980) 489.
32. T. EKSTRÖM, in *Mat. Res. Soc. Symp. Proc. (Materials Research Society, USA, 1993) Vol. 287*, p. 121.
33. S. BOSKOVIC, K. J. LEE and T. Y. TIEN, in *Mat. Res. Soc. Symp. Proc. (Materials Research Society, USA, 1993) Vol. 287*, p. 373.
34. C. ZHANG, W. Y. SUN and D. S. YAN, in "Key Engineering Materials, Vol. 161-163" (Trans Tech Publications, Switzerland, 1999) p. 239.
35. M. MITOMO, T. SHIOGAI, H. YOSHIMATSU and M. TSUTSUMI, *Yogyo-Kyokai-Shi.* **93** (1985) 69.

*Received 26 August 1999  
and accepted 22 June 2000*